

Supplemental Material

Bridging the reality gap in quantum devices with physics-aware machine learning

D.L. Craig[†],¹ H. Moon[†],¹ F. Fedele,¹ D.T. Lennon,¹ B. van Straaten,¹ F. Vigneau,¹
 L.C. Camenzind,² D.M. Zumbühl,² G.A.D. Briggs,¹ M.A. Osborne,³ D. Sejdinovic,⁴ and N. Ares^{*3}
¹*Department of Materials, University of Oxford, Parks Road, Oxford OX1 3PH, United Kingdom*
²*Department of Physics, University of Basel, 4056 Basel, Switzerland*
³*Department of Engineering Science, University of Oxford, Parks Road, Oxford OX1 3PJ, United Kingdom*
⁴*Department of Statistics, University of Oxford, 24-29 St Giles, Oxford OX1 3LB, United Kingdom*

As discussed in the main text, we provide a detailed schematic of the CNN architectures used for \mathcal{F}_U and \mathcal{F}_D in Figure S1. Examples of 2D scans and their human expert labels regarding the presence of a double quantum dot are shown in Figure S2. An additional set of example posterior disorder samples generated using a simulated device where the true disorder is known is shown in Figure S3.

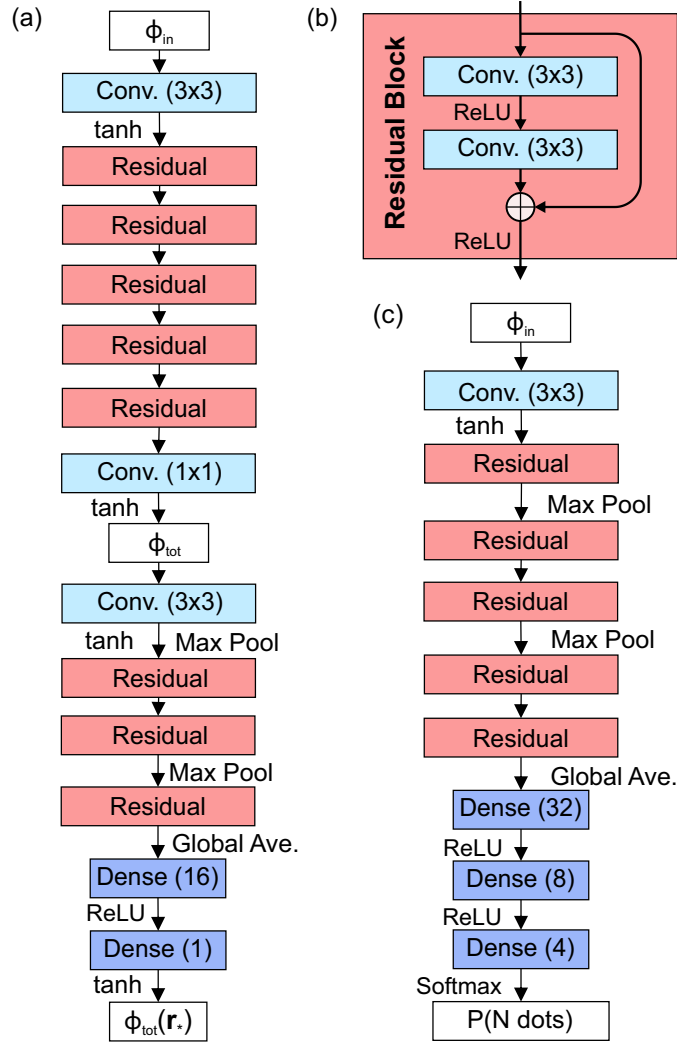


Figure S1. The neural networks used to compute U^* and classify dots. Text to the left and right of the arrows indicates the activation function applied and dimension reduction processes respectively. (a) Structure of \mathcal{F}_U beginning with the 2D normalised input potential ϕ_{in} , to the self-consistent potential ϕ_{tot} , and finally to the minimax value $\phi_{tot}(\mathbf{r}_*)$. All convolutional units have 32 channels. (b) Schematic of a residual block as used in \mathcal{F}_U and \mathcal{F}_D . The number of channels is preserved through a residual block. (c) Structure of \mathcal{F}_D beginning with the normalised input potential, with a probability distribution for the number of dots as the output. All convolutional units have 64 channels, and dots are classified using one-hot encoding for $\{0, 1, 2, 3\}$ dot classes.

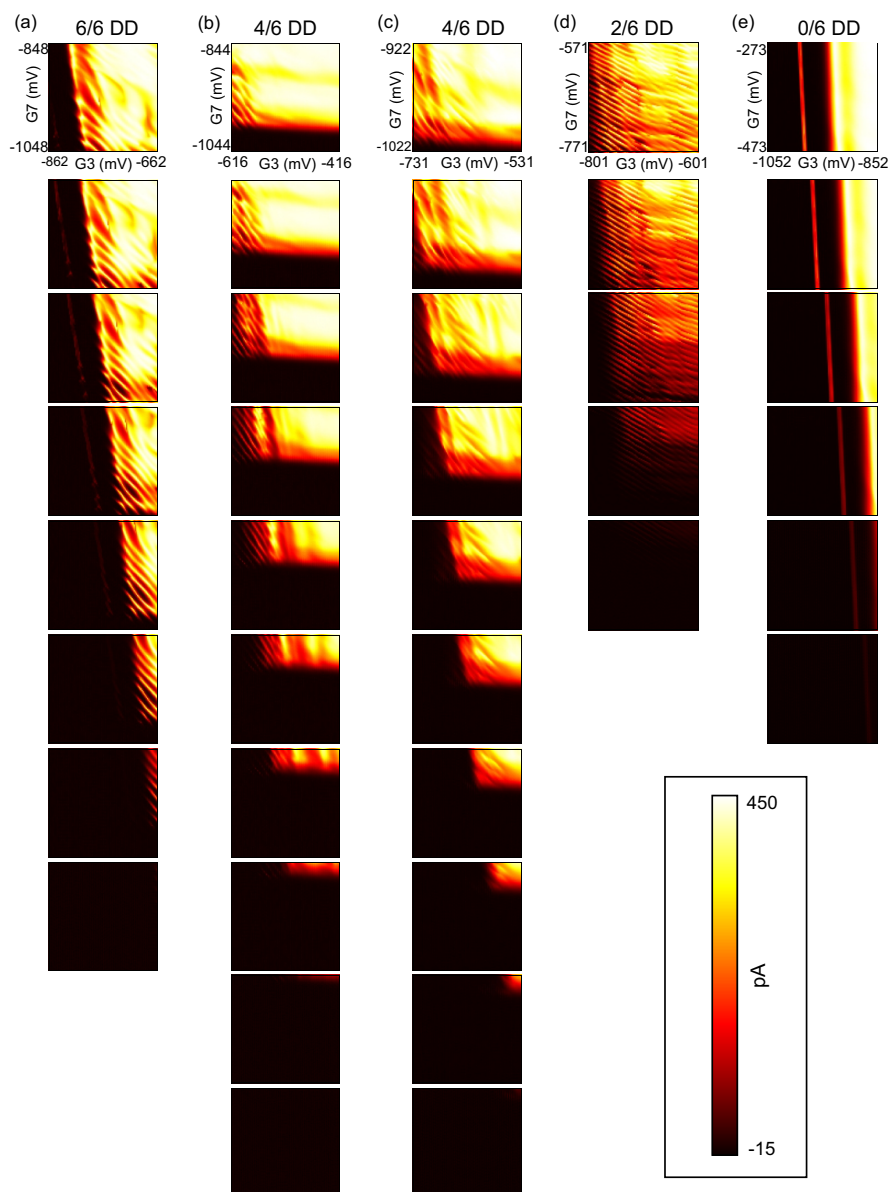


Figure S2. Each column (a)-(e) is a set of 2D current scans taken using a vector accepted by the filtering process discussed in the main text. Each scan is a $200\text{mV} \times 200\text{mV}$ window over gates G3 and G7, with the original 7-dimensional voltage vector at the centre. The magnitude of R (as defined in the main text) is increased by 13.3mV from one row to the next. The axes of the first scan in each column are labelled to indicate the range of voltage values considered. The colour scale shared by all plots is shown in the box. The result of human expert labels is indicated at the top of each column. For example, ‘4/6 DD’ indicates that 4 out of 6 labellers considered a double dot to exist in the set of current scans. The vectors (a)-(d) were only accepted using posterior disorders and (e) was only accepted using random disorders. Some vectors were accepted by both random and posterior disorders, but not the examples shown.

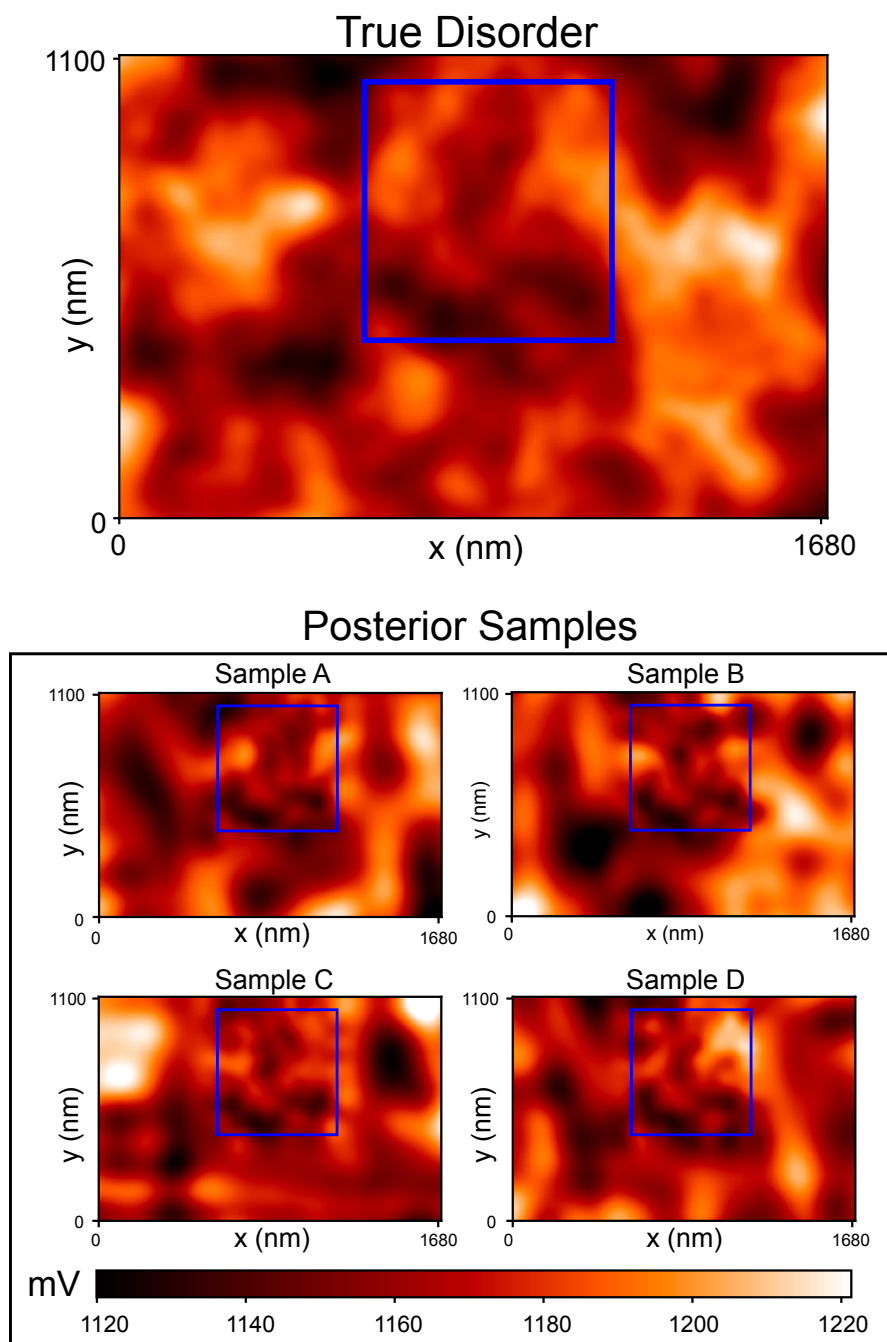


Figure S3. The true disorder and 4 randomly selected posterior disorder samples for an iteration of the inference algorithm on a simulated device. The true disorder is generated using the electrostatic model with randomly located donor ions. The blue box on each disorder potential indicates the region spanned by the optimised inducing points. The posterior disorder samples are the same resolution as the true disorder, (134x206). The posterior disorders have more detailed features within the box, and qualitative similarities with the true disorder can be observed. All plots share the same scale, as shown at the beneath the posterior samples.